npj | genomic medicine

Article

Published in partnership with CEGMR, King Abdulaziz University

https://doi.org/10.1038/s41525-025-00471-x

# Identification of cryptic breakpoints through single-tube long fragment read whole genome sequencing based on preimplantation genetic testing



Lu Jiang[1,2,6], Zhuoyao Mai[3,4,6], Jiguang Peng[1,6], Tao Du[3,4], Weifeng Wang[1], Xiran Chen[3,4], Chen Jiang[1], Yantao Luo[1,2], Hui Chen[3,4], Lijie Song[1,2], Nengyong Ouyang[3,4] ✉, Chao Chen[1,2,5] ✉ & Ping Yuan[3,4] ✉

This study utilized single-tube long fragment read whole genome sequencing (stLFR WGS) to identify cryptic chromosomally balanced translocations in preimplantation genetic testing (PGT), aiming to improve outcomes for couples experiencing recurrent pregnancy loss (RPL). G-banded karyotyping initially revealed normal results for Family 1 and a reciprocal translocation for Family 2. However, PGT's low-coverage WGS uncovered recurrent copy number variations (CNVs) that contradicted the initial findings. Further analysis using stLFR WGS and Sanger sequencing precisely located the breakpoints, revealing a balanced translocation between chromosomes 7 and 13 in Family 1's male and a complex translocation involving chromosomes 9, 10, and 11 in Family 2's female. By selecting non-carrier embryos for transfer, the study resulted in successful births of healthy infants. These findings highlight the critical role of PGT in detecting concealed chromosomal rearrangements and demonstrate stLFR WGS as an effective diagnostic tool for breakpoint identification, significantly impacting reproductive decisions for couples with cryptic balanced translocations and RPL.

Chromosomally balanced translocations involve the exchange of segments originating from two or more non-homologous chromosomes[1]. These translocations are among the most prevalent chromosomal rearrangements, with an estimated occurrence rate of 0.16–0.2%[2,3]. Typically, carriers of chromosomally balanced translocations exhibit a normal phenotype, as the total gene copy number remains unchanged and gene expression is not adversely affected. However, in rare instances, such translocations have been linked to various diseases, particularly when the breakpoints result in gene truncation. In the context of reciprocal translocations, during meiosis, at least 18 different gamete types can be produced. Of these, only one is normal, another is balanced, while the remaining gametes exhibit unbalanced chromosomal alterations, manifesting as derivatives of terminal sequence duplications and deletions adjacent to the breakpoint[4,5]. The production of unbalanced gametes increases the likelihood of infertility, recurrent pregnancy loss (RPL), and the birth of fetuses with anomalies in carriers[6]. In contrast, complex translocations, which involve at least three breakpoints on two or more chromosomes, pose a greater risk of RPL and abnormal fetal development compared to reciprocal translocations[7].

Karyotyping analysis is conditionally recommended for couples with a history of RPL as a means of screening for parental chromosome rearrangement[8]. The conventional G-banding karyotyping method can detect a wide array of chromosome rearrangements, including translocation[9]. However, its resolution limit ranges between 5 and 10 Mb, subject to the specific genomic region and assay conditions, not to mention the variability in diagnostic rates among different practitioners[10]. The resolution of chromosome microarray analysis (CMA) can reach 100 kb, but it is incapable of identifying balanced translocation[11]. Fluorescence in situ hybridization (FISH) necessitates prior knowledge of the target region as well as specifically designed probe[12,13]. Therefore, cryptic balanced translocations, which involve the relocation of small chromosomal fragments, can often elude detection through standard cytogenetic and CMA methods. This oversight is primarily attributable to several factors: (1) the translocated segments are similar in size and exhibit indistinguishable banding patterns;

[1]BGI Genomics, Shenzhen, 518083, China. [2]Clin Lab, BGI Genomics, Tianjin, 300308, China. [3]Department of Obstetrics and Gynecology, Sun Yat-Sen Memorial Hospital of Sun Yat-Sen University, Guangzhou, 510120, China. [4]Guangdong Provincial Clinical Research Center for Obstetrical and Gynecological Diseases, Guangzhou, 510120, China. [5]College of Life Sciences, University of Chinese Academy of Sciences, Beijing, 100049, China. [6]These authors contributed equally: Lu Jiang, Zhuoyao Mai, Jiguang Peng. ✉e-mail: ouyny@mail.sysu.edu.cn; chenchao4@bgi.com; kekeyp1983@163.com

(2) the translocations occur in regions of low genetic activity, particularly near the subtelomeric areas; (3) the size of the translocated segments approaches or falls below the resolution threshold of the analytical techniques employed[14,15]. Additionally, the presence of complex translocations, characterized by multiple breakpoints and cryptic segments, further complicates the detection process, posing significant challenges to conventional analytical methodologies. Nevertheless, the identification of copy number variations (CNV) can provide insights into the likelihood of detecting cryptic balanced translocations through CMA of chorionic villus samples and preimplantation genetic testing for aneuploidy (PGT-A) in blastocysts[6,15].

Recently, whole genome sequencing (WGS) has been utilized to detect balanced translocations and inversions with single-base resolution. However, its effectiveness is somewhat limited due to the read length and the occurrence of repetitive DNA sequences at specific breakpoints. These limitations can obscure crucial genomic details, thus affecting the precision and reliability of the sequencing outcomes in identifying such chromosomal rearrangements[9,16]. In contrast, single-tube long fragment read (stLFR) whole genome sequencing leverages the incorporation of identical barcode sequences into subfragments of an extended DNA molecule, thereby facilitating the analysis of long DNA sequences. Research indicates that stLFR is effective in detecting complex structural variants. We presented the first report of two couples with RPL who successfully pinpointed their cryptic translocation breakpoints using stLFR WGS, informed by the results of PGT on embryonic samples. It demonstrated the potential of stLFR technology in revealing intricate chromosomal structural anomalies that underlie preimplantation genetic testing for structural rearrangement (PGT-SR).

## Results

In Family 1, experiencing multiple adverse pregnancy outcomes, the couple's karyotype analyses via G-banding indicated normal chromosomal structures. Subsequent MLPA analyses of miscarried tissues hinted at possible duplications or deletions on chromosome 7 and 13. To enhance their chances of a successful pregnancy and a healthy baby, the couple was suggested to undergo the in vitro fertilization and embryo transfer (IVF-ET) with PGT-A utilizing low-coverage WGS (Supplementary Table 1). Out of 13 biopsied blastocysts, PGT-A identified a range of chromosomal conditions: 6 embryos showed duplication or deletion of 7q36.2–q36.3, 4 were euploid without mosaicism, 2 displayed euploid with mosaicism, and one was aneuploidy with mosaicism (Fig. 1a, b).

The PGT-A results of 6 embryos implied that one of the couples was likely to be a cryptic balanced translocation carrier. To verify the accuracy of the results, stLFR WGS and high-coverage WGS for the parent-embryo haplotype analysis were performed (Supplementary Table 1). From the 13,512,128 detected SNPs, there were 953 informative SNPs available for haplotype analysis, and we identified that the balanced haplotype was linked to the breakpoints of chromosome 7 and 13 from the husband (Table 1, Fig. 1c). Based on our PGT strategy, we focused on 4 euploid without mosaicism and 1 euploid with low-level mosaicism embryos, and found 4 normal embryos (E03, E08, E11, and E12) and one balanced translocation embryo (Fig. 1c).

Furthermore, in comparison with normal 46,XY karyotype, the cryptic breakpoints at chr7:153732372 and chr13:111186281 were validated by Sanger sequencing (Supplementary Table 2, Fig. 3a, b). Based on the above results, only 3 embryos were both euploids without mosaicism and normal

a

| Family | Embryo No. | Day | Scoring | PGT-A results | Outcome | PGT-SR results |
|---|---|---|---|---|---|---|
| 1 | E01 | 5 | 4BB | del(7q36.2-q36.3,5.30M) | D | NA |
| | E02 | 5 | 4BB | del(7q36.2-q36.3,5.64M) | D | NA |
| | E03 | 5 | 4BA | mos(+8[37%]) | F | Normal (mosaic) |
| | E04 | 5 | 4AB | dup(7q36.2-q36.3,5.37M) | D | NA |
| | E05 | 5 | 4BB | dup(7q36.2-q36.3,5.54M) | D | NA |
| | E06 | 5 | 4BB | mos(-19[55%]) | D | NA |
| | E07 | 5 | 4AB | del(7q36.2-q36.3,5.19M) | D | NA |
| | E08 | 5 | 3AB | Euploid | F | Normal |
| | E09 | 5 | 4AB | dup(7q36.2-q36.3,5.48M) | D | NA |
| | E10 | 5 | 4BA | Euploid | F | Balanced translocation |
| | E11 | 5 | 4AB | Euploid | F | Normal |
| | E12 | 6 | 4BC | Euploid | F | Normal |
| | E13 | 6 | 4BB | -16,mos(+X[44%],+Y[45%],-6[59%],+10[30%],+12[44%],+17[30%],-18[35%],+22[47%]) | D | NA |

c

| ID | Chr. | Position | Husband | | Wife | | Embryo E03 | | Embryo E08 | | Embryo E10 | | Embryo E11 | | Embryo E12 | |
|---|---|---|---|---|---|---|---|---|---|---|---|---|---|---|---|---|
| rs39158 | 7 | 153669134 | A | G | A | A | A | A | A | A | G | A | A | A | A | A |
| rs10952455 | 7 | 153670199 | T | C | T | T | T | T | T | T | C | T | T | T | T | T |
| rs39156 | 7 | 153670448 | G | A | G | G | G | G | G | G | A | G | G | G | G | G |
| rs39133 | 7 | 153682815 | G | A | A | A | G | A | G | A | A | A | G | A | G | A |
| rs149487087 | 7 | 153684094 | T | C | T | T | T | T | T | T | C | T | T | T | T | T |
| rs57301263 | 7 | 153740215 | A | G | G | G | A | G | A | G | G | G | A | G | A | G |
| rs4725524 | 7 | 153789707 | A | C | A | A | A | A | A | A | C | A | A | A | A | A |
| rs12154225 | 7 | 153795009 | C | T | C | C | C | C | C | C | T | C | C | C | C | C |
| rs11762853 | 7 | 153819262 | A | C | A | A | A | A | A | A | C | A | A | A | A | A |
| rs4360211 | 7 | 153821935 | C | A | C | C | C | C | C | C | A | C | C | C | C | C |
| rs9555758 | 13 | 111709867 | A | G | G | G | A | G | A | G | G | G | A | G | A | G |
| rs9555759 | 13 | 111709899 | T | A | A | A | T | A | T | A | A | A | T | A | T | A |
| rs9559951 | 13 | 111709953 | G | A | A | A | G | A | G | A | A | A | G | A | G | A |
| rs4773314 | 13 | 111710177 | C | T | T | T | C | T | C | T | T | T | C | T | C | T |
| rs2183852 | 13 | 111710581 | A | G | G | G | A | G | A | G | G | G | A | G | A | G |
| rs2150894 | 13 | 111710632 | C | G | G | G | C | G | C | G | G | G | C | G | C | G |
| rs2150893 | 13 | 111710675 | G | A | A | A | G | A | G | A | A | A | G | A | G | A |
| rs9559955 | 13 | 111712097 | G | C | C | C | G | C | G | C | C | C | G | C | G | C |
| rs9559974 | 13 | 111742028 | C | T | T | T | C | T | C | T | T | T | C | T | C | T |
| rs1240273882 | 13 | 111793212 | C | G | G | G | C | G | C | G | G | G | C | G | C | G |

b

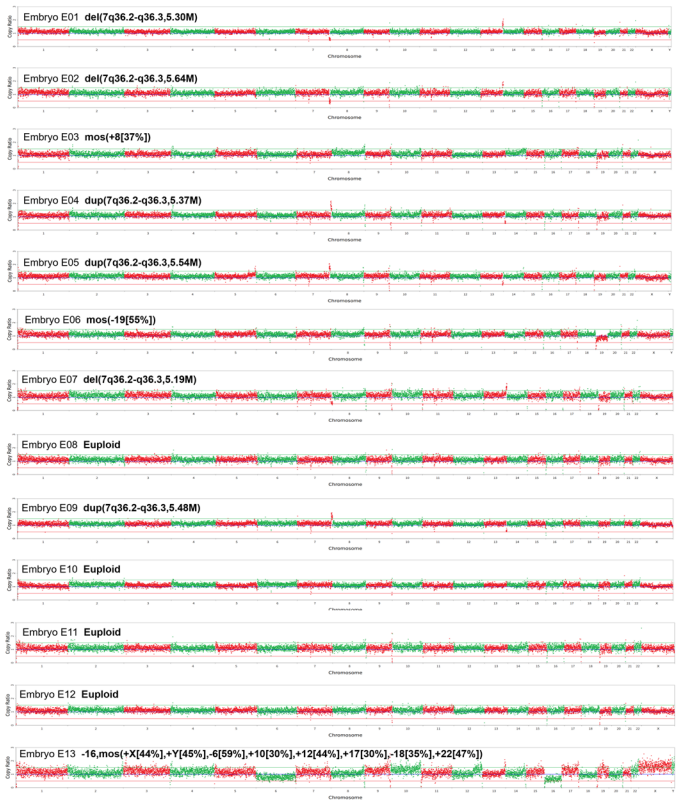


**Fig. 1 | Preimplantation genetic testing for aneuploidies and structural rearrangements (PGT-A and PGT-SR) results of biopsied embryos in Family 1.** **a** Comprehensive Analysis of PGT-A and PGT-SR Results of 13 Embryos. Among the 13 embryos examined, 3 were found to be euploid without translocation (E08, E11, E12), 1 embryo exhibited euploid with a balanced translocation (E10), and 1 embryo showed no translocation but displayed mosaicism. The remaining embryos exhibited abnormal copy number variations (CNVs). D discarded embryos; F, frozen embryos; NA, not available. **b** Scatter diagrams illustrating CNVs detected in the 13 embryos by low-coverage whole genome sequencing. **c** Results of linkage analyses (partial SNP sites excerpted) of the blastocyst-stage embryos capable of transplantation. Twenty SNP markers linked to the breakpoints were selected to identify the balanced haplotype and the normal haplotype in each embryo. Blue bars indicate the maternal normal haplotype, red bars indicate the paternal balanced haplotype, and green bars indicate the paternal normal haplotype. ID, reference SNP cluster ID; Chr., chromosome number; Position, genomic location.

**Table 1 | Results of chromosome balanced translocation detection using single-tube long fragment read whole genome sequencing**

| Family | Chromosome | Region | Breakpoint position | Haplotype Block | No. of Informative SNPs* |
|---|---|---|---|---|---|
| Husband in family 1 | chr7 | 7p36.2 | 153732372 | 152156179–154266719 | 58 |
| | chr13 | 13q34 | 111186281 | 100951856–112353444 | 895 |
| Wife in family 2 | chr9 | 9p21 | 28963900 | 27041315–28962818 | 351 |
| | chr9 | 9p21 | 28974360 | 27041315–28962818 | 351 |
| | chr9 | 9p13 | 35323542 | 34699598–37179855 | 157 |
| | chr10 | 10q23 | 95505222 | 94958183–97182128 | 109 |
| | chr10 | 10q23 | 107382817 | 106665432–109757837 | 244 |
| | chr11 | 11q12 | 39402584 | 38517134–40737956 | 243 |
| | chr11 | 11q12 | 39402653 | 38517134–40737956 | 243 |
| | chr11 | 11p12 | 39402655 | 38517134–40737956 | 243 |

No., number; *Informative SNPs are defined as those that are heterozygous in the carrier individual and homozygous in the carrier's partner.

a

| Family | Embryo No. | Day | Scoring | PGT-A results | Outcome | PGT-SR results |
|---|---|---|---|---|---|---|
| 2 | E01 | 5 | 3BC | del(10q23.33-q26.3,39.78M),dup(9p21.1-p13.3,5.40M),dup(11p15.5-p12,39.09M) | D | NA |
| | E02 | 5 | 4BC | dup(9p21.1-p13.3,6.25M),dup(10p15.3-q23.33,95.23M),dup(10q25.1-q26.3,27.98M) | D | NA |
| | E03 | 5 | 4BB | del(10q23.33-q25.1,11.65M),dup(9p21.1-p13.3,6.48M) | D | NA |
| | E04 | 5 | 3BC | Euploid | F | Normal |
| | E05 | 6 | 3BC | del(4q28.3-q35.2,51.37M),del(10q25.1-q26.3,27.73M),dup(11p15.5-p12,38.38M) | D | NA |
| | E06 | 6 | 3BC | -18,+22,del(6p25.3-p24.1,12.93 M),del(10q23.33-q25.1,11.84M),dup(9p21.1-p13.3,6.10M) | D | NA |

b

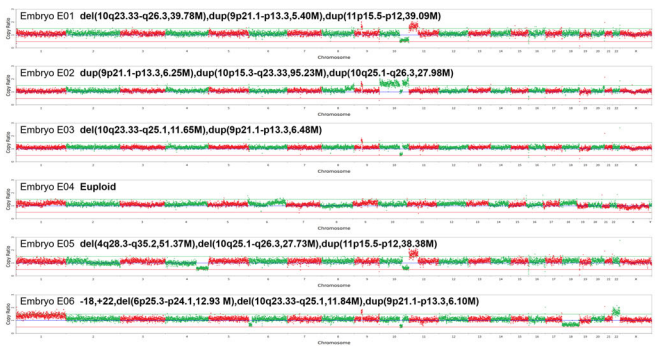


c

| ID | Chr. | Position | Husband | | Wife | | Embryo E04 | |
|---|---|---|---|---|---|---|---|---|
| rs2039995 | 9 | 27813045 | C | C | A | C | A | C |
| rs7020846 | 9 | 28403443 | C | C | T | C | T | C |
| rs6476065 | 9 | 28403813 | T | T | C | T | C | T |
| rs10118885 | 9 | 28460340 | G | G | A | G | A | G |
| rs10117978 | 9 | 28496596 | T | T | C | T | C | T |
| rs650058 | 10 | 95378547 | A | A | G | A | G | A |
| rs11187554 | 10 | 95379998 | A | A | G | A | G | A |
| rs1223306 | 10 | 95380790 | A | A | G | A | G | A |
| rs473934 | 10 | 95391936 | T | T | A | T | A | T |
| rs616522 | 10 | 95395247 | G | G | A | G | A | G |
| rs11594268 | 10 | 95531617 | A | A | A | G | A | A |
| rs7099034 | 10 | 95545378 | T | T | T | C | T | T |
| rs10736084 | 10 | 95551702 | T | T | T | C | T | T |
| rs829223 | 10 | 95715764 | A | A | T | A | T | A |
| rs829225 | 10 | 95718474 | G | G | A | G | A | G |
| rs1896187 | 11 | 39028170 | A | A | C | A | C | A |
| rs6485049 | 11 | 39030072 | A | A | G | A | G | A |
| rs2861584 | 11 | 39030578 | A | A | G | A | G | A |
| rs2114464 | 11 | 39035644 | C | C | T | C | T | C |
| rs7102065 | 11 | 39053694 | T | T | C | T | C | T |
| rs10742521 | 11 | 39987682 | T | T | C | T | C | T |
| rs10742525 | 11 | 40039945 | T | T | C | T | C | T |
| rs10768571 | 11 | 40040893 | T | T | A | T | A | T |
| rs6485174 | 11 | 40044520 | C | C | T | C | T | C |
| rs1531449 | 11 | 40045913 | A | A | G | A | G | A |

**Fig. 2 | Preimplantation genetic testing for aneuploidies and structural rearrangements (PGT-A and PGT-SR) results of biopsied embryos in Family 2.** **a** Comprehensive Analysis of PGT-A and PGT-SR Results of 6 embryos. Among the 6 embryos examined, only 1 were found to be euploid without translocation (E04), and the rest are with abnormal copy number variations (CNVs). D discarded embryos, F frozen embryos, NA not available. **b** Scatter diagrams illustrating CNVs detected in the 6 embryos by low-coverage whole genome sequencing WGS. **c** Results of linkage analyses (partial SNP sites excerpted) of the blastocyst-stage embryos. Twenty-five SNP markers linked to the breakpoints were selected to identify the balanced haplotype and the normal haplotype in each embryo. Blue bars indicate the paternal normal haplotype, red bars indicate the maternal balanced haplotype, and green bars indicate the maternal normal haplotype. ID, reference SNP cluster ID; Chr., chromosome number; Position, genomic location.

karyotype without translocation (E8, E11, E12), as shown in Fig. 1a. Among these, embryo E11 was chosen for transfer due to its superior morphological grading, led to a confirmed clinical pregnancy. Following successful prenatal amniocentesis diagnosis, a healthy infant was born at 38 weeks 1 day of gestation, with postnatal stLFR WGS corroborating the child's normal karyotype (Supplementary Fig. 1a and Supplementary Fig. 2a, b).

In family 2, the couple had a history of multiple pregnancy loss, but genetic information of the abortus was unavailable. Karyotype analysis showed that the male had a normal karyotype with G-banding, while the female was a balanced translocation carrier(46,XX,t(10;11)(q24.3;p12)). In order to have a healthy baby, the couple was suggested to undergo IVF-ET with PGT-A by low-coverage WGS (Supplementary Table 1). By analyzing 6 embryos, only one showed euploid without mosaicism. The remaining 5 embryos displayed intricate karyotypes marked by duplications and/or deletions of segments on chromosome 11 and chromosome 10, consistent with the anticipated maternal balanced translocation. Noteworthy findings included the deletion spanning from 4q28.3 to q35.2 in embryo E05, alongside sporadic occurrences such as the deletions of 6p25.3 to p24.1, Trisomy 22, and monosomy 18 in embryo E6. However, considerable attention was drawn to the discovery that 4 embryos shared a common duplication spanning from 9p21.1 to p13.3 (Fig. 2a, b). It was inferred that one of the couples likely carried a translocation involving chromosome 9. In

order to gain deeper insights into the chromosome rearrangement and pinpoint the exact breakpoints, we conducted stLFR WGS and high-coverage WGS for the parent-embryo haplotype analysis (Supplementary Table 1). Among the 11,938,932 detected SNPs, 1104 informative SNPs were available for haplotype analysis. We identified that the balanced haplotype was associated with 8 breakpoints spanning chromosome 9, 10, and 11 from the wife (Table 1 and Fig. 3c). Carrier analysis of chromosomal balanced translocation was conducted for the only euploid embryo E04 based on the WGS data.

These breakpoints, located at chr9:28963900, chr9:28974360, chr9:35323542, chr10:95505222, chr10:107382817, chr11:39402584, chr11:39402653, and chr11:39402655, were subsequently validated by Sanger sequencing (Supplementary Table 2, Fig. 3c, d). Fortunately, E04 was transferred finally due to its availability as the only viable option. Prenatal diagnosis was performed on the mother at 18 weeks and 5 days of gestation, with both G-banding and CMA results showing normal findings. A healthy boy was delivered via cesarean section at 36 weeks and 2 days of gestation. Cord blood was collected at birth for stLFR WGS analysis, confirming the newborn's normal karyotype.

## Discussion

Herein, we present the successful application of single-tube long fragment read whole genome sequencing as a viable method for detecting cryptic balanced translocations for the first time. Our findings also underscored the significance of PGT for couples with RPL, particularly in uncovering cryptic balanced translocations. In cases where translocation carriers were initially overlooked during karyotyping or challenges were encountered in the cytogenetic analysis of pregnancy tissues, PGT-A proves to be a valuable tool for uncovering cryptic karyotypes. Furthermore, the use of stLFR WGS techniques provided additional confirmation of cryptic breakpoints and chromosomal structural abnormalities in embryos.

Chromosomally balanced translocations carriers are at significantly increased risk of RPL due to generation of unbalanced gametes. It is reported that unbalanced sperm rates of male carriers ranged from 30.3 to 72.2%[17], and unbalanced oocytes rate of female carriers was 39.7%[18]. On the other hand, research data demonstrated that prevalence of balanced translocation carriers among RPL couples was up to 7.2%, much higher than the estimated 0.16–0.2% of population[9]. Therefore, guidelines on recurrent pregnancy loss recommend RPL couples to undergo karyotyping[8,19]. The G-banding analysis indicated normal chromosomal structures in Family 1. In contrast, the female in Family 2 was identified as a carrier of reciprocal translocation carrier (46,XX,t(10;11)(q24.3;p12)). Subsequent PGT-A findings revealed that 6 out of 13 biopsied embryos from Family 1 exhibited either duplication or deletion at 7q36.2–q36.3. This observation, combined with their history of recurrent pregnancy loss (RPL) and MLPA-confirmed duplications/deletions on chromosomes 7 and 13, suggested that one partner might harbor a reciprocal translocation. In Family 2, beyond the maternal reciprocal translocation between chromosomes 10 and 11, four out of six embryos demonstrated duplication at 9p21.1–p13.3, raising suspicions of additional cryptic breakpoints. Furthermore, subsequent stLFR WGS analysis verified the actual karyotypes of the suspected carriers, facilitating accurate identification of the cryptic breakpoints. This precision enabled a thorough haplotype analysis and the selection of viable embryos for transfer. The stLFR WGS findings indicated that the cryptic translocation segments were either comparable to or significantly smaller than 5 Mb. This discovery elucidated why G-banding, with its 5–10 Mb resolution limit, was inadequate for detecting these specific chromosomal rearrangements, emphasizing the value of advanced genomic sequencing in diagnosing complex genetic conditions accurately.

Regarding the utilization of various techniques for detecting balanced translocations, FISH is adept at identifying submicroscopic deletions and duplications within genomic regions spanning 100 kb or larger, rendering it suitable for translocation detection near telomeres. However, this method necessitates the use of fluorescent probes specifically tailored to the region of interest. Furthermore, FISH lacks the precision to pinpoint exact breakpoints and proves ineffectual in identifying novel rearrangements[8,10,11]. Low-coverage WGS has been acknowledged for uncovering additional chromosomal abnormalities in 4.0% of couples afflicted with RPL. Nevertheless, its primary constraints are rooted in the limited read length and the complexity posed by repetitive DNA sequences at certain breakpoints[9]. Previous reports have also indicated that certain short-read sequencing can tackle similar issues. Peters et al. firstly adopt long fragment reading (LFR) technology, successfully achieving typing of embryonic monoploidy. However, this technique is complex to perform experimentally, and compared to standard whole genome sequencing, the overall sensitivity for high-confidence SNV detection has decreased by 15%[20]. Furthermore, in the recent study conducted by Janssen et al., the authors introduce WGS-PGT, a comprehensive clinical whole genome sequencing approach applicable to all forms of preimplantation genetic testing. While this technology represents a significant advancement, it still encounters specific challenges in detecting small duplications[21]. Single-molecule sequencing excels in uncovering structural variations, but has several drawbacks: higher sequencing error rates, increased costs, complex library preparation[22].

However, stLFR WGS emerges as a proficient technique, utilizing cobarcoding of subfragments from long genomic DNA molecules with a single unique barcode. This method eliminates the need for DNA amplification of the original long fragments, thereby minimizing representation bias[23]. stLFR employs short-read sequencing platforms to analyze these long DNA fragments, effectively reducing the errors commonly associated with single-molecule sequencing. As stLFR integrates seamlessly with short-read sequencing platforms, it aligns well with existing laboratory workflows and analysis pipelines. This compatibility is particularly beneficial for laboratories already equipped with short-read sequencing technologies, as it negates the necessity for substantial modifications to their existing setups to incorporate stLFR. For individuals who are cryptic balanced translocation carriers experiencing RPL, the integration of PGT-A and stLFR WGS, both anchored in short-read sequencing technologies, serves a dual purpose. These methodologies not only identify the breakpoints with precision but also facilitate the screening of embryos to ascertain those with a normal karyotype. This strategic approach ensures the selection of viable embryos, enhancing the prospects for successful live birth outcomes in affected couples.

Although the presence of a small, unbalanced chromosomal segment might not directly precipitate fetal demise, a substantial body of evidence has established that cryptic chromosomal rearrangements can lead to a spectrum of disorders, including leukemia[24–26], developmental and epileptic encephalopathy[27], Angelman syndrome[28], intrauterine growth restriction and major structural anomaly of fetus[29], and mental retardation[30,31]. In cases where balanced translocation carriers are not identified during initial karyotyping, these cryptic rearrangements may go undetected until a pattern of adverse pregnancy outcomes or the manifestation of related diseases in siblings raises concern. However, we outline an approach to assist these carriers by identifying recurrent duplications or deletions in specific segments through PGT-A analysis of biopsied embryos. A pertinent study involving 48 couples with unexplained RPL and normal karyotypes revealed that, upon undergoing PGT-A, 17 couples presented multiple embryos exhibiting similar structural variations. Subsequentmate-pair sequencing analysis (an optimized protocol of next-generation sequencing) identified 13 balanced translocation carriers among these 17 couples[14]. This finding underscores the significance of an "unbalanced translocation-like" pattern in PGT-A result as an indicator of the underlying karyotype anomalies in RPL-affected parents, providing insights into their recurrent miscarriage. By selecting the appropriate technological intervention, in this case, stLFR WGS, clinicians can accurately identify chromosomal breakpoints and confirm the true karyotypes, thereby enhancing genetic counseling and the precision of subsequent PGT approaches.

In conclusion, our research revealed that two couples, harboring cryptic balanced translocations and experiencing RPL, achieved live births through the integration of PGT-A and PGT-SR and stLFR WGS methodologies. This study not only highlights the critical role of PGT in detecting cryptic chromosomal rearrangements in embryos but also introduces stLFR WGS as an innovative diagnostic approach for pinpointing specific

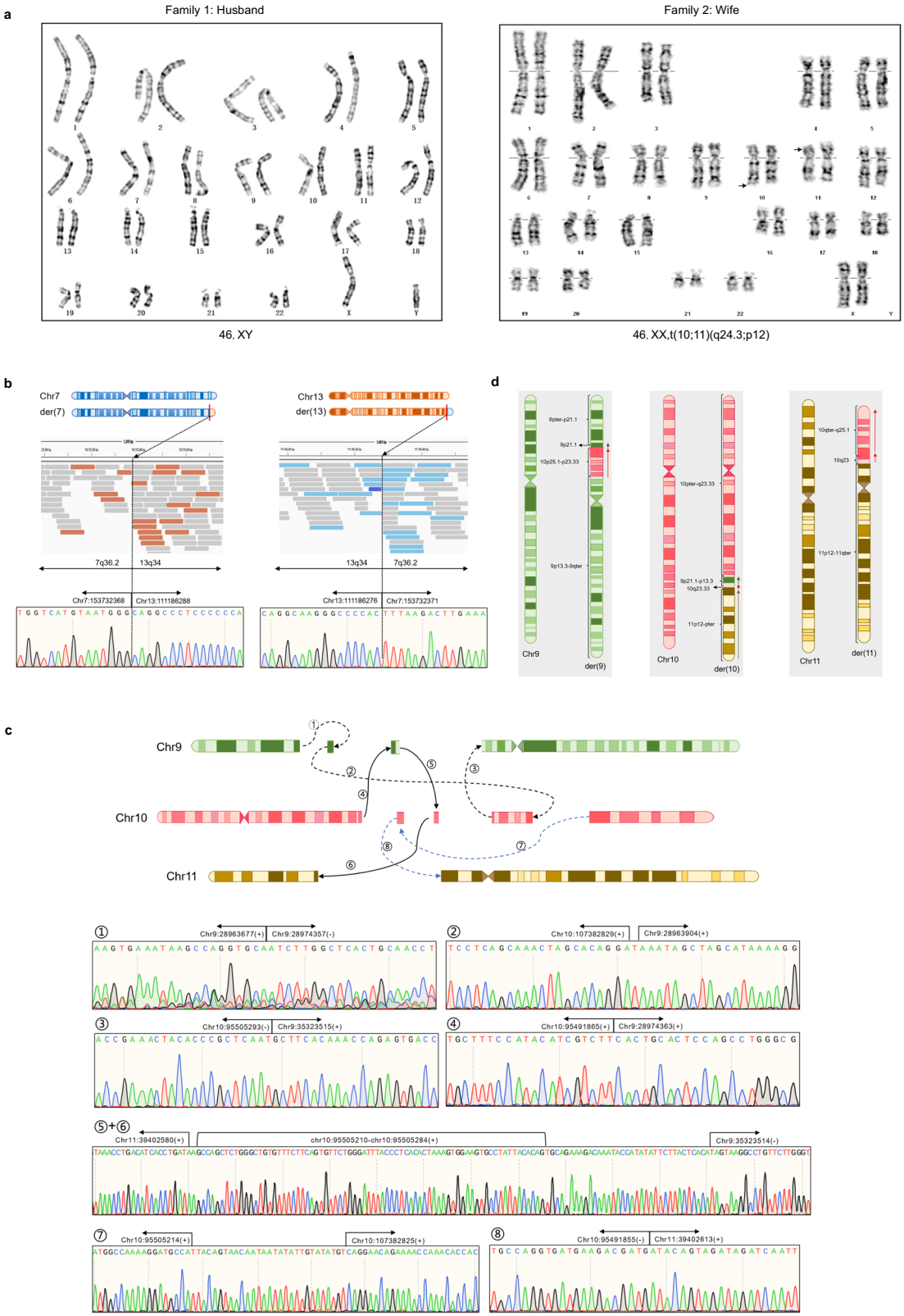


**Fig. 3 | Karyotype analysis of Family 1 and Family 2 with different techniques.** **a** Previous G-banded chromosomes of the husband in Family 1 (left) and the wife in Family 2 (right). **b** Identification of cryptic breakpoints on chromosomes 7 and 13 in the husband of Family 1. Breakpoints are precisely located using single-tube long fragment read whole genome sequencing (stLFR WGS) and confirmed through Sanger sequencing. Arrows above indicate the breakpoints. **c** Identification of cryptic breakpoints on chromosomes 9, 10, and 11 in the wife of Family 2. Breakpoints are accurately pinpointed using stLFR WGS and validated through Sanger sequencing. Arrows above indicate the breakpoints. **d** A diagram illustrating the derived chromosomes 9, 10 and 11 of the wife in Family 2.

breakpoints. Moreover, the application of high-coverage WGS for PGT-SR offered identifiable insights into balanced and normal karyotypes. Consequently, stLFR WGS emerges as a promising tool, poised to significantly influence the reproductive decisions of couples with cryptic balanced translocations seeking interventions for RPL.

## Methods

### Ethics approval

The study was approved by the Human Research and Ethics Committee at Sun Yatsen Memorial Hospital of Sun Yat-sen University and was conducted in accordance with the Declaration of Helsinki. Informed consent was obtained from all participants for their enrollment and the publication of results without revealing the participant's identity.

### Patients

Family 1, a Chinese family, suffered two miscarriages at 8 weeks of gestation. The abortuses were confirmed to have duplications and/or deletions of both chromosome 7 and 13 by multiplex ligation-dependent probe amplification (MLPA) analysis (Supplementary Table 3). The 30-year-old female in this family exhibited normal ovarian reserve and basic hormone levels appropriate for her age (Supplementary Table 3). Salpingography and hysteroscopy demonstrated bilateral patent fallopian tubes and a normal uterine cavity. No abnormalities were identified in the sperm and blood tests of her 28-year-old husband. Considering their strong desire to have a healthy infant, this couple underwent karyotype testing (G-banding) and requested preimplantation genetic testing (PGT).

Family 2 was another Chinese family that had encountered four miscarriages following the term birth of a healthy infant in 2008. G-banding karyotype analysis revealed that the 34-year-old female carried a reciprocal translocation (46,XX,t(10;11)(q24.3;p12)), while her 38-year-old husband had a normal karyotype (46,XY). Unfortunately, genetic information regarding the miscarriages was not available. Fertility evaluation demonstrated normal ovarian reserve and baseline hormone levels in the female. No abnormalities were detected in the sperm and blood tests of her husband. After receiving comprehensive genetic counseling, this couple made the informed decision to reduce the risk of miscarriage through PGT.

### Oocyte retrieval, intracytoplasmic sperm injection, and blastocyst biopsy

Informed consent for PGT was obtained prior to the initiation of controlled ovarian hyperstimulation (COH) using gonadotropin (Gn)-releasing hormone (GnRH) agonist long protocol (Supplementary Table 3). Oocyte retrieval was conducted under ultrasound guidance 36 h after the administration of human chorionic gonadotropin (hCG). Intracytoplasmic sperm injection (ICSI) was performed on metaphase II (MII) oocytes. Fertilization assessment was carried out approximately 18 hours post-injection by observing the presence of two pronuclei (2PN) and the second polar body (PB2). Embryos were cultured using sequential media, specifically G1-plus/G2-plus (Vitrolife, Sweden). In accordance with the Gardner grading system for blastocyst assessment[32], blastocysts graded between 3 and 6, with either the inner cell mass (ICM) or trophectoderm (TE) graded above C, were deemed suitable for biopsy. TE biopsy was performed on either day 5 or day 6 by employing zona drilling with a laser, and a small sample of biopsied TE cells (5–8 cells) was extracted and collected for genetic analysis.

### Whole genome sequencing

The biopsied TE cells (TEs) were utilized for whole genome amplification (WGA). In brief, the TEs underwent degenerate oligonucleotide-primed PCR-based WGA using a GenomePlex® Single Cell WGA Kit (Sigma, USA). The resulting DNA products were quantified using the dsDNA HR assay on a Qubit fluorometer (Thermo Fisher Scientific, Waltham, MA, USA). Subsequently, library construction for these DNA products was carried out using the MGIEasy FS DNA library prep set (MGI, China). Both the DNA amplification and sequencing library preparations adhered to the manufacturer's protocols. The prepared DNA libraries were then subjected to sequencing on a MGISEQ-2000 platform (MGI, China) employing a sequencing strategy of 0.3× WGS SE35 or 15× WGS PE100.

The original data underwent filtration and alignment to the human reference genome 19 (Hg19) using SOAP 2.2.1 (http://soap.genomics.org.cn) to obtain the initial alignment results. Duplicate reads were subsequently removed, and the mapped reads were sorted based on their chromosome coordinates. To eliminate bias from WGA, corrections for GC bias and population biases were applied. Based on the comparative results, the sequencing depth and coverage for each sample were quantified. CNV segments were detected using a circular binary segmentation algorithm[33].

### Genomic DNA extraction and stLFR WGS

Peripheral blood genomic DNA (gDNA) were extracted from each couple, while umbilical cord blood gDNA were extracted from fetus, using MagAttract HMW DNA kit (QIAGEN, Germany) for each sample. The DNA concentration of gDNA was determined using the aforementioned method. Subsequently, the stLFR libraries of these gDNA products were following the standard protocol, employing the MGIEasy stLFR Library Preparation kit (MGI, China). Briefly, the transposon-inserted DNAs were hybridized in a single tube with magnetic beads containing multi-copy molecular barcodes, following the DNA double-strand complementation principle. The resulting DNA libraries were then subjected to sequencing using the MGISEQ-2000RS High-throughput Sequencing Set (stLFR) (PE100) (MGI, China).

The original data underwent filtration and alignment against hg19 using the Long Ranger pipeline (v.2.2.2) to obtain the initial alignment results. The annotated files containing barcodes and phasing information were generated, serving as the reference haplotypes of the family. Duplicate reads were subsequently removed, and base quality recalibration was performed using GATK (v4.0.3)'s HaplotypeCaller (https://gatk.broadinstitute.org/hc/en-us). This allowed for the analysis of single nucleotide polymorphisms (SNPs) and insertions and deletions (indels) to identify variations. Evaluation metrics, such as average sequencing depth, coverage, and other relevant indicators for both the genome and phase set, were also computed based on the alignment results.

### Precise breakpoint detection by Sanger sequencing

We utilized stLFR WGS to initially identify the breakpoint regions of the reciprocal translocations. Subsequently, sequences encompassing the putative breakpoint regions were confirmed through polymerase chain reaction (PCR) employing junction-spanning primers. This was followed by the precise localization of the breakpoints using Sanger sequencing (primer sequences are available in Supplementary Table 4).

### Study design for cryptic breakpoint

As depicted in Fig. 4, the initial low-coverage WGS PGT-A analysis revealed that the couple's embryos exhibited the same unbalanced translocation characteristics as those typically observed in embryos from carriers with significant balanced translocations. To investigate the possibility of an undetected cryptic reciprocal translocation in the parents, we employed stLFR WGS. The breakpoint regions of the mutual translocation were initially pinpointed using stLFR WGS, followed by Sanger sequencing to precisely map the breakpoints.

Furthermore, we conducted a detailed analysis of selected single nucleotide polymorphisms (SNPs) within the balanced translocation carriers and their partners using stLFR WGS. Informative SNPs were identified when those upstream and downstream of a breakpoint were heterozygous in the carriers and homozygous in their partners[34]. By leveraging these informative SNPs and high-coverage WGS data from the embryos, we successfully distinguished normal blastocysts from those carrying balanced translocations.

### Prenatal and postnatal diagnosis

Both families underwent recommended amniocentesis in the second trimester to further assess the fetal genetic results. Karyotypes and CNVs of the embryos selected for transfer were confirmed through G-banding and CMA of amniotic fluid cells. Subsequently, at birth, the infants' karyotypes were

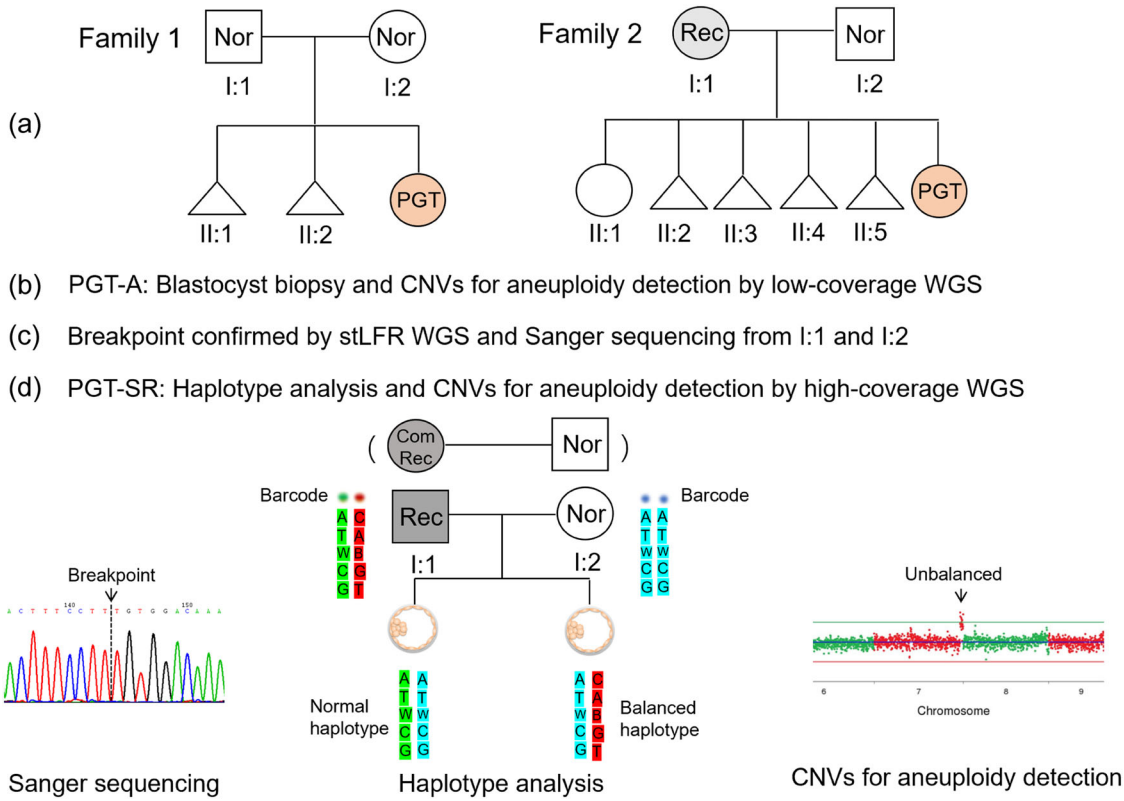


**Fig. 4 | Workflow for identifying cryptic translocation breakpoints and pre-implantation genetic testing (PGT). a** Pedigree across two generations. Filled symbols represent individuals with chromosomal diseases detected through G-banding, while open symbols indicate individuals with a normal karyotype via G-banding. Circles and squares denote females and males, respectively. Triangles indicate aborted embryos with uncertain gender. **b** PGT-A through blastocyst biopsy and low-coverage whole genome sequencing (WGS) for copy number variation (CNV) analysis. CNV analysis results reveal recurrent duplications or deletions in specific segments, suggesting possible cryptic chromosomal translocations in the affected couples. **c** Breakpoints identified by single-tube long fragment read whole genome sequencing (stLFR WGS) and confirmed by Sanger sequencing. Peripheral blood samples from individuals I:1 and I:2 in both families were used for confirmation. **d** PGT-SR analysis through haplotype analysis and CNV detection for aneuploidy by high-coverage WGS of blastocyst biopsy. Haplotype construction is based on heterozygous sites in the affected parent (translocation carrier) and homozygous sites in the unaffected parent (non-carrier). In the haplotype, A, T, C, and G represent different SNP markers; W denotes the wild-type allele, and B indicates the balanced allele.

meticulously verified once more using single-tube long fragment read (stLFR) whole genome sequencing of cord blood samples.

## Data availability

The data that support the findings of this study are available from the corresponding author upon reasonable request.

Received: 29 July 2024; Accepted: 28 January 2025;
Published online: 21 February 2025

## References

1. Gupta, N., Dalvi, R., Koppaka, N. & Mandava, S. Balanced reciprocal translocation: multiple chromosome rearrangements in an infertile female. *J. Hum. Reprod. Sci.* **12**, 72–74 (2019).
2. Jacobs, P. A., Browne, C., Gregson, N., Joyce, C. & White, H. Estimates of the frequency of chromosome abnormalities detectable in unselected newborns using moderate levels of banding. *J. Med. Genet.* **29**, 103–108 (1992).
3. Van Dyke, D. L., Weiss, L., Roberson, J. R. & Babu, V. R. The frequency and mutation rate of balanced autosomal rearrangements in man estimated from prenatal genetic studies for advanced maternal age. *Am. J. Hum. Genet.* **35**, 301–308 (1983).
4. Oda, S. et al. A complex rearrangement between APC and TP63 associated with familial adenomatous polyposis identified by multimodal genomic analysis: a case report. *Front. Oncol.* **13**, 1205847 (2023).
5. Xu, P. et al. OGM and WES identifies translocation breakpoints in PKD1 gene in an polycystic kidney patient and healthy baby delivered using PGT. *BMC Med. Genomics* **16**, 285 (2023).
6. Morin, S. J., Eccles, J., Iturriaga, A. & Zimmerman, R. S. Translocations, inversions and other chromosome rearrangements. *Fertil. Steril.* **107**, 19–26 (2017).
7. Pellestor, F. et al. Complex chromosomal rearrangements: origin and meiotic behavior. *Hum. Reprod. Update* **17**, 476–494 (2011).
8. RPL, E. G. G. O. et al. ESHRE guideline: recurrent pregnancy loss: an update in 2022. *Hum. Reprod. Open* **2023**, hoad002 (2023).
9. Dong, Z. et al. Genome sequencing explores complexity of chromosomal abnormalities in recurrent miscarriage. *Am. J. Hum. Genet.* **105**, 1102–1111 (2019).
10. Miller, D. T. et al. Consensus statement: chromosomal microarray is a first-tier clinical diagnostic test for individuals with developmental disabilities or congenital anomalies. *Am. J. Hum. Genet.* **86**, 749–764 (2010).
11. Schaaf, C. P., Wiszniewska, J. & Beaudet, A. L. Copy number and SNP arrays in clinical diagnostics. *Annu. Rev. Genomics Hum. Genet.* **12**, 25–51 (2011).
12. Knight, S. J. & Flint, J. Perfect endings: a review of subtelomeric probes and their use in clinical diagnosis. *J. Med. Genet.* **37**, 401–409 (2000).
13. Zhang, S. et al. Detection of cryptic balanced chromosomal rearrangements using high-resolution optical genome mapping. *J. Med. Genet.* **60**, 274–284 (2023).

14. Li, S. et al. Identification of cryptic balanced translocations in couples with unexplained recurrent pregnancy loss based upon embryonic PGT-A results. *J. Assist. Reprod. Genet.* **41**, 171–184 (2024).
15. Ou, J. et al. Identification and interruption of inheritance of familial cryptic translocations: a case report. *Mol. Genet. Genom. Med.* **12**, e2356 (2024).
16. Treangen, T. J. & Salzberg, S. L. Repetitive DNA and next-generation sequencing: computational challenges and solutions. *Nat. Rev. Genet.* **13**, 36–46 (2011).
17. Del Llano, E. et al. Sperm meiotic segregation analysis of reciprocal translocations carriers: we have bigger FISH to fry. *Int. J. Mol. Sci.* **24**, 3664 (2023).
18. Durban, M. et al. PGD in female carriers of balanced Robertsonian and reciprocal translocations by first polar body analysis. *Hum. Reprod. Update* **7**, 591–602 (2001).
19. Regan, L., Rai, R., Saravelos, S. & Li, T.-C. & Gynaecologists, o.b.o.t.R.C.o.O.a. Recurrent Miscarriage.Green-top Guideline No. 17. *Br. J. Obstet. Gynaecol.* **00**, 1–31 (2023).
20. Peters, B. A. et al. Detection and phasing of single base de novo mutations in biopsies from human in vitro fertilized embryos by advanced whole-genome sequencing. *Genome Res.* **25**, 426–434 (2015).
21. Janssen, A. E. J. et al. Clinical-grade whole genome sequencing-based haplarithmisis enables all forms of preimplantation genetic testing. *Nat. Commun.* **15**, 7164 (2024).
22. Warburton, P. E. & Sebra, R. P. Long-read DNA sequencing: recent advances and remaining challenges. *Annu. Rev. Genomics Hum. Genet.* **24**, 109–132 (2023).
23. Wang, O. et al. Efficient and unique cobarcoding of second-generation sequencing reads from long DNA molecules enabling cost-effective and accurate sequencing, haplotyping, and de novo assembly. *Genome Res.* **29**, 798–808 (2019).
24. Ahmed, N., Ketterling, R. P., Nowakowski, G. S., Dasari, S. & Feldman, A. L. RNAseq identification of FISH-cryptic BCL6::TP63 rearrangement in ALK-negative anaplastic large-cell lymphoma. *Histopathology* **81**, 275–278 (2022).
25. Panagopoulos, I. et al. Fusion of ETV6 with an intronic sequence of the BAZ2A gene in a paediatric pre-B acute lymphoblastic leukaemia with a cryptic chromosome 12 rearrangement. *Br. J. Haematol.* **133**, 270–275 (2006).
26. Mohebnasab, M. et al. Cytogenetically cryptic acute promyelocytic leukemia: a diagnostic challenge. *Int. J. Mol. Sci.* **24**, 13075 (2023).
27. Orlando, V. et al. A complex genomic rearrangement resulting in loss of function of SCN1A and SCN2A in a patient with severe developmental and epileptic encephalopathy. *Int. J. Mol. Sci.* **23**, 12900 (2022).
28. Burke, L. W. et al. Familial cryptic translocation resulting in Angelman syndrome:implications for imprinting or location of the Angelman gene? *Am. J. Hum. Genet* **58**, 777–784 (1996).
29. Chen, M. et al. Subtelomeric rearrangements and 22q11.2 deletion syndrome in anomalous growth-restricted fetuses with normal or balanced G-banded karyotype. *Ultrasound Obstet. Gynecol.* **28**, 939–943 (2006).
30. Granzow, M. et al. Multiplex FISH telomere integrity assay identifies an unbalanced cryptic translocation der(5)t(3;5)(q27;p15.3) in a family with three mentally retarded individuals. *Hum. Genet.* **107**, 51–57 (2000).
31. Kleefstra, T. et al. Identification of an unbalanced cryptic translocation between the chromosomes 8 and 13 in two sisters with mild mental retardation accompanied by mild dysmorphic features. *Eur. J. Hum. Genet.* **8**, 637–640 (2000).
32. Gardner D. K., S. W. In vitro culture of human blastocysts. *Toward Reproductive Certainty: Fertility and Genetics Beyond 1999*. (Parthenon Publishing, London, 1999) pp. 378–388.
33. Yin, X. et al. Massively parallel sequencing for chromosomal abnormality testing in trophectoderm cells of human blastocysts. *Biol. Reprod.* **88**, 69 (2013).
34. Zhang, S. et al. The establishment and application of preimplantation genetic haplotyping in embryo diagnosis for reciprocal and Robertsonian translocation carriers. *BMC Med. Genomics* **10**, 60 (2017).


## Acknowledgements

This study was supported by the National Key Research and Development Program of China (2019YFA0801403 and 2023YFC2705604), the National Natural Science Foundation of China (81801431), Beijing Health Promotion Association-2022 Young and Middle-aged Doctors Research (BJHPA-2022-SHZHYXZHQNYJ-LCH-011), Natural Science Foundation of Guangdong Province (2023A1515010515), Guangzhou Basic and Applied Basic Research Foundation (2023A04J2081) and Sun Yat-Sen Memorial Hospital Clinical Research 5010 Program (SYS-5010-202410).We appreciate Miss Ye Wang for her invaluable help in karyotype information and all participants involved in this study.

## Author contributions

P. Y., C. C., N. OY., Z. M., and L. J. designed the whole study. P. Y., X. C. and H. C. recruited patients. S. L. collected samples and variant verification and data curation. T. D. contributed to Karyotype validation. L.J, J.P, W.W, C.J, Y.L and L.S completed sequencing, data analysis, and variant interpretation. P. Y., Z. M., and N. OY. collected and analyzed the PGT results. Z. M., L. J., P. Y., C. C., and N. OY. wrote the paper. All authors approved the final version of the paper.

## Competing interests

The authors declare no competing interests.

## Additional information

**Supplementary information** The online version contains supplementary material available at https://doi.org/10.1038/s41525-025-00471-x.

**Correspondence** and requests for materials should be addressed to Nengyong Ouyang, Chao Chen or Ping Yuan.